2019 SECED Conference
Earthquake risk and engineering towards a resilient world
9-10 September 2019, Greenwich, London

SEISMIC BEHAVIOUR AND DESIGN OF STEEL REDUCED BEAM SECTION CONNECTIONS

D.V. BOMPA[1], A.Y. ELGHAZOULI[2]

Abstract: *This study describes detailed numerical investigations into the inelastic cyclic response of beam-column assemblages of moment frames incorporating reduced beam section (RBS) welded connections. Detailed three-dimensional nonlinear finite element procedures are validated against results of selected tests from a series of three large scale experimental tests. After gaining confidence in the ability of the numerical models to predict closely the full inelastic response, a number of numerical investigations are carried out. Particular emphasis is given to the influence of key material and geometric parameters on the balance of energy dissipation between the panel zone and the reduced beam zones. The results of the parametric studies enable direct assessments regarding the contribution of the main dissipative components to the inelastic performance of RBS moment connections, as a function of the main geometric and material parameters. Key observations from the numerical simulations, which are relevant for the design and assessment for such configurations are highlighted within the discussions with particular focus on European seismic design guidelines.*

Introduction

Steel moment frames have typically been designed with rigid full-strength connections in welded or welded/bolted configurations and need to be provided with sufficient overstrength such that dissipative zones develop in the beams (Elghazouli, 2015). The poor performance of such connections under previous seismic events, produced by excessive strain demands leading to brittle fractures, initiated a series of studies in which alternative configurations were sought. These investigations focused on extending the lifetime of existing structures under extreme loading trough retrofit, as well as to develop new design procedures for incorporation in standards (SAC, 1995). Besides possible connection strengthening methods such as the addition of haunches, continuity plates or other alternatives, another strategy consists of weakening the beam by producing a Reduced Beam Section (RBS). Early configurations involved trimming the flanges in a trapezoidal or straight cut (Plumier, 1990). However, the SAC report (1995) indicated that the straight cut RBS can result in stress concentrations at the corners of the cut. The trapezoidal cuts lead to a uniformly distributed yielding pattern, yet fractures have been reported, initiating at the corners at the returns of the tapered section (Chen et al., 1996). In contrast, the radius cut RBS, later adopted in North American and European codified procedures, tends to exhibit a more ductile behaviour, minimising the fracture hazard (Engelhardt et al., 1996).

Results of a two-stage experimental programme including RBS connections and corresponding conventional counterparts indicate that the non-RBS connections experienced a premature fracture at the flange whilst those with RBS showed much more stable hysteretic behaviour, with plastic hinges forming in the RBS regions (Popov et al., 1996). Additional shake-table tests on two one-story frames, with and without RBS, indicated significant differences in terms of the hysteretic response of connections, with those provided with RBS developing more stable and higher energy dissipation capacity than their conventional counterparts (Chen et al., 1996). Experimental assessments undertaken by Lee at al. (2005) indicated that strong and medium panel zone (PZ) specimens with a welded web connection demonstrate satisfactory ductile behaviour, whilst those with a bolted web connection exhibit poor performance due to premature brittle fracture of the beam flange at the weld access hole. Additional comments from that study suggested that specimens with strong PZ experience more significant beam local buckling and permanent deformation because of the inelastic behaviour being concentrated in the reduced section. Although not recommended (Lee at al., 2005), RBS connections with very weak PZ can

[1] Postdoctoral Research Associate, Imperial College London, UK, d.bompa@imperial.ac.uk
[2] Professor, Imperial College London, UK, a.elghazouli@imperial.ac.uk

demonstrate good performance exhibiting large total storey drifts without strength degradation and excellent energy dissipation (Jones at al., 2002). All yielding would occur in the PZ while the RBS regions remain largely elastic, ultimately failing by low-cycle induced fast fracture, at large drift levels.

It is widely accepted that reliable failure modes of RBS connections are characterised by extensive yielding at the RBS, followed by limited yielding of the PZ and ultimately local flange buckling at the RBS. The reduction in the beam flange may not only produce local flange buckling, but also early local buckling in the web compared to normal beams (Jones et al., 2002). Such effects are typically reduced or eliminated in a composite configuration of the connections when a reinforced concrete slab is present (Zhang & Ricles, 2006). The presence of a composite slab offers bracing to the beam and reduces the lateral displacement of the bottom flange, as well as reduce the out of plane column rotation observed in RBS connections without slabs (Chi & Uang, 2002). These studies contributed directly to the North American prequalification requirements of steel connections for seismic resistant steel structures (AISC-358), which are limited to sections up to 900 mm in depth and 450 kg/m in weight. Practical needs for heavy section sizes for high rise structures, initiated studies for the extension of these prequalification limits to large jumbo steel profiles (Chen and Tu, 2004; Li et al., 2018, Bogdan et al., 2019). The latter study, part of a wider European research project (Landolfo et al., 2018) indicates that compact sections with relatively low depth-to-web thickness ratios develop unreliable response with yielding occurring almost concomitantly at the beam web of the RBS and the PZ.

Although the RBS concept was initially introduced in Europe, the number of studies incorporating European sections is relatively limited (Figure 1a). For example, results from a test on a connection incorporating HEB300 column and straight cut with rounded corners IP450 RBS beam show that weld failure occurred after only 4 cycles (50% loss of capacity) due to high stress concentration in the welding detail, where localised plastic strains may exist (Plumier et al., 2000). Elsewhere, tests on HEB300 columns connected to HEA180A and HEA240 radius cut RBS, point out to the inadequacy of the RBS design procedure implemented in the Eurocode 8 when using European profiles (Pachoumis et al. 2009). Specimens with a smaller reduction of the beam flange, compliant with the codified procedure, may experience severe yielding and fracture in the vicinity of the column face at the bottom flange of the beam, outside of the RBS region (Pachoumis et al. 2010). Moreover, bolted end plate connections, incorporating HEA160 beam with reduced section and HEB300 column, develop an acceptable level of rotation capacity (Sofias et al., 2014). It is worth noting that all test specimens mentioned above, made of European sections, were provided with horizontal continuity plates extending from the beam flanges at the web column panel, hence all had a strong PZ.

Although numerous studies were carried out on beam-to-column RBS connections incorporating US steel profiles, there is a dearth of investigations involving connections made of European sections. Existing tests are limited to a single column configuration provided with a strong PZ and HEA160-240 and IPE450 beams. Available non-linear numerical studies on RBS connections provided with European profiles are limited to strong PZ or beam-to-concrete filled steel tubes (e.g Zhang and Ricles 2006b; Vulcu et al, 2017). As observed, connections made of European sections that employ a balanced PZ design are lacking. To this end, this study investigates the non-linear response of edge RBS IPE beam-to-HEB column connections subjected to cyclic loading. After undertaking numerical validation studies on three specimens from various experimental programmes, non-linear parametric investigations are carried out to provide detailed insights into the physical behaviour of such connections. Within the parametric investigations, parametric assessments are carried out to assess the contribution of the main connection components to the global connection response, including stiffness, strength and ductility as well as energy dissipation and hysteretic response. Finally, key observations which are relevant for the design and assessment for such configurations are highlighted within the discussions.

Numerical procedures and validation

The numerical simulations described in this paper were carried out using the non-linear finite element (FE) program ABAQUS (DSS, 2014). The numerical procedures described below were validated against three specimens with various configurations from three different experimental studies. Firstly, Specimen C3B in Figure 1b which is provided with a HEB300 column and an IPE450 beam, provided with a straight cut with rounded corners RBS, was modelled (Plumier et al., 2000). The second specimen (RBSa) considered (Figure 1c) consists of HEB300 column and

HEA180 beam (Pachoumis et al., 2010). To consider the response of connections made of large sections, the third modelled configuration was an RBS connection (SP2) depicted in Figure 1d, incorporating jumbo profiles (Bogdan et al., 2019). Specimens RBSa and SP2 developed reliable ductility levels with an expected sequence of yielding, triggered by inelastic strains at the RBS followed by buckling at the bottom flange. In contrast, Specimen C3B failed at the weld due to high stress concentrations at the column face. The details of these connections, including the dimensions of the RBS cuts, are listed in Table 1.

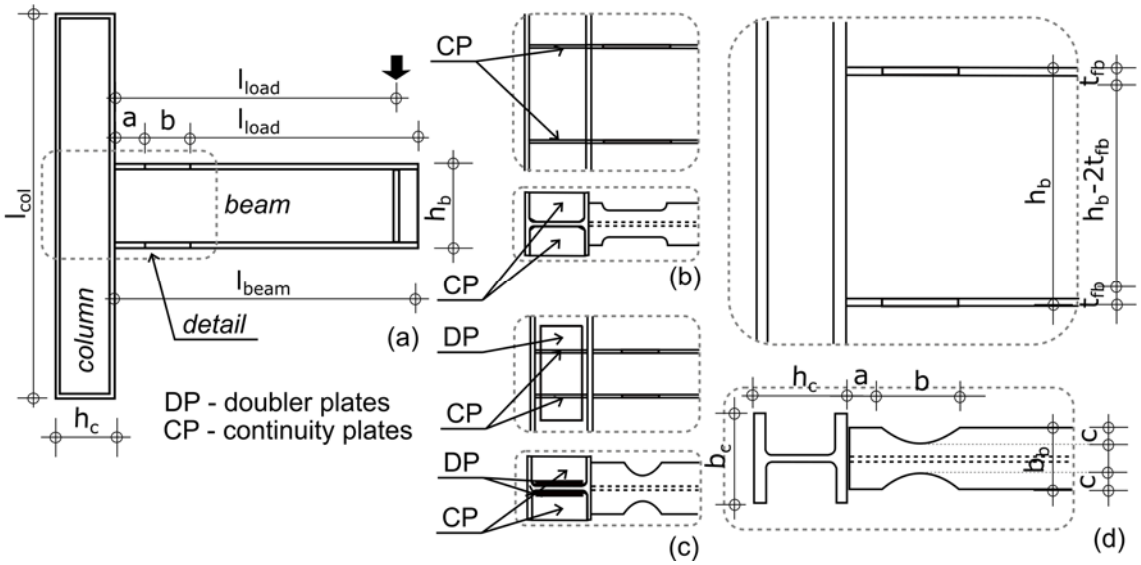

Figure 1 a) Details of an RBS specimen; Connection details for: a) C3B, b) RBSa, c)SP2

	Column		Beam		RBS			PZ	
Spec.	Section	$b_c \times h_c \times t_{wc} \times t_{fc}$ (mm)	Section	$b_b \times h_b \times t_{wb} \times t_{fb}$ (mm)	a (mm)	b (mm)	c (mm)	t_{cp} (mm)	t_{dp} (mm)
C3B	HEB 300	300×300×11×19	IPE450	50×190×9.4×14.6	50	300	35*	15	-
RBSa	HEB 300	300×300×11×19	HEA180	171×180×6×9.5	144	128.3	36	10	12
SP2	W360×509	446×416×39.1×62.7	W1100×343	1090×400×18× 31	201	709	68.3	-	-

Table 1 Specimen details

Three-dimensional (3D) models of RBS connections adopted eight node brick elements (C3D8R). Extruded solid elements from steel sections representing the column were connected to the beams using tie constraints. Special attention was given to the characteristics of the RBS region and the column PZ by considering the exact dimensions taken from the experimental specimens. Multi-point constraints connected to reference points were assigned with pinned boundary conditions to the ends of the column. Cyclic displacements were applied to reference points that are connected to the actuator position through constraints simulating faithfully the experimental time history. Mesh sensitivity studies were undertaken to assess the element size influence on the hysteretic response. These indicated that a relatively coarse mesh restricts a reliable inelastic strain propagation within the RBS and that local buckling effects are not captured. On the other hand, a fine mesh within the RBS and column PZ (l_m≈15-20 mm), combined with l_m≈30-40 mm outside of the critical regions offered reliable deformations and strains, as described in subsequent sections. A minimum of two mesh rows per flange thickness offered a good balance in terms of computational time and reliability of results, whilst a much larger number of rows significantly increased the analysis time and reduced the ability of the model to capture local effects, primarily due to hourglass phenomena (Bompa and Elghazouli, 2017). The Newton-Raphson approach was adopted for the numerical integration procedure. The steel material properties were modelled using a plastic multilinear kinematic hardening constitutive representation in which the material properties obtained from coupon testing were accounted for.

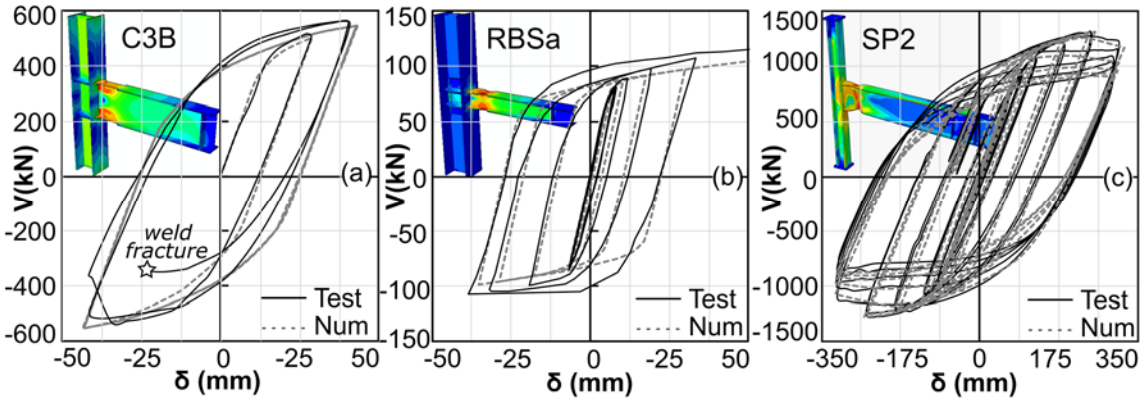

Figure 2 Numerical validation – for Specimen: a) C3B, b) RBSa, C) SP2

Figures 2a-c presents the relationship of the load versus beam tip deflection or at the load application points, whilst Figure 3a-c illustrates the Mises strain maps at maximum displacement. The results indicate reliable prediction in terms of elastic stiffness, yielding characteristics and deformations, and relatively good predictions of the hysteretic response for all specimens. It is worth noting that the modelling procedure adopted does not account for the welds, and the beam element is tied to the column face. As mentioned above, Specimen C3B had limited ductility due to failure by weld fracture; and as welds are not explicitly modelled, such failure modes cannot be directly predicted. However, for this specimen, all key performance parameters resulting from numerical simulations are in good agreement with the test results (Figure 2a).

The hysteretic response, stiffness and yield characteristics are also correctly predicted for Specimen RBSa. The predicted capacity associated with key displacement points is slightly lower in comparison to the test capacity, primarily due to a single available material stress-strain curve adopted for all connection elements (Figure 2b). It is widely accepted that due to manufacturing procedures, the flanges and webs of the same steel profile have distinct strength characteristics although they are produced from the same steel billet. Hence, this has an impact on the predicted structural response. On the other hand, for Specimen SP2, the numerical results closely capture the initiation of flange buckling and plastic development in the RBS region and PZ, primarily since the material characteristics of all connection components (i.e. beam flange and web, column flange and web), obtained from coupon tests, were used as input for modelling.

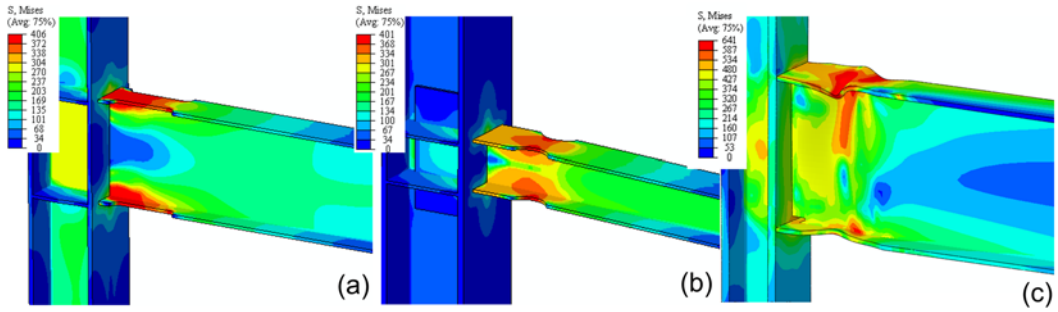

Figure 3 Mises strain maps at maximum displacement for a) C3B, b) RBSa, c) SP2

Additionally, the strain maps in Figure 3 point out to a response governed by extensive yielding at the RBS for all specimens, yet relatively distinct in behaviour. Connection C3B developed extensive yielding at the RBS, but with significant stress concentrations at the column face. This suggests that the RBS cut type adopted (Figure 1b) may not ensure a ductile connection response, primarily due to extreme demands on the welds due to stress localisation (Figure 3a). Stresses at the PZ are about 70% of those at the RBS, indicating a significant contribution from the web column panel to the global energy dissipation. For connection RBSa, the presence of doubler and continuity plates at the column maintained the PZ stresses at around 25% of those from the RBS. As observed from Figure 3b, the connection had a reliable response with extensive yielding developing at the RBS flanges and web, hence a strong PZ. As mentioned above, Connection SP2 reached a reliable response which was ultimately governed by flange and web yielding and buckling at the RBS (Figure 3c). As described above, the strength, deformational

response and failure modes obtained from the numerical simulations were generally in good agreement with the corresponding test measurements. Having gained confidence in the modelling procedures through the three validations described above, detailed parametric studies were then carried out, as outlined below.

Parametric investigations

A total of 20 models were constructed using the numerical procedures described above. Four of the connections were extracted from a 6 storey-4 bays moment resisting frame (MRF) designed according to the Eurocodes, whilst for the remaining 16, the members were changed incrementally. For brevity, only 6 representative models are described and analysed herein. The considered seismic resistant structural system of MRF was a perimeter seismic resistant system in which the inner bays are pinned and designed for gravity loads only. The MRF span was 6.00 m, whilst the storey height was 3.50 m. The connections, listed in Table 2, incorporate beams and columns with sizes varying in the range IPE360-IPE550 and HEB240-HEB360, respectively. The connection assemblages included l_{col}=3.0 m long columns and l_{beam}=1.5 m long beams with the load application points at l_{load}=1.32 mm, which corresponds to the zero-bending region. A radius cut RBS was considered, in which the distance from the column to RBS is a=0.6×b_b, the RBS length b=0.75×h_b and the RBS depth b=0.2×b_b (see notations in Figure 1 and Eurocode 8).

All connection components were assigned the same steel material properties: yield strength f_y=355 MPa, ultimate strength f_u=490 MPa and ultimate strain ε_u=0.18. The connections were initially subjected to monotonic loading to obtain the yield displacement δ_y, which was then used to construct the cyclic loading procedure. The yield displacement obtained from monotonic loading varied in the range δ_y=8-12 mm depending on the section sizes of the connection components. The applied displacements in the cyclic procedure were based on one cycle at 0.25, 0.5, 0.75 and 1.0×δy, followed by three cycles at 2.0×δy and (2+2n)×δy up to failure, where δy is the average lateral yield deformation δ_y=10 mm and n=1, 2, 3, etc. Results from the cyclic models allow a direct assessment of the moment-rotation M-θ curves (Figure 4), yield and ultimate characteristics, post-peak degradation and the contribution of the main connection components to the ultimate response. Bending moments M were assessed at the column face from the reaction forces obtained at reference points. For the global behaviour, chord rotations θ are assessed from beam displacements δ at the reaction points.

Model	Beam		RBS	Column	
	Section	h_b×b_b×t_{wb} ×t_{fb} (mm)	a×b×c (mm)	Section	h_c×b_c×t_{wc}×t_{fc} (mm)
IV-1	IPE360	360×170×8×13	102×270×34	HEB360	360×300×13×23
IV-3	IPE360	360×170×8×13	102×270×34	HEB280	280×280×11×18
IV-4	IPE360	360×170×8×13	102×270×34	HEB240	240×240×10×17
III-1	IPE400	400×180×8.6×14	108×300×36	HEB360	360×300×13×23
III-2	IPE400	400×180×8.6×14	108×300×36	HEB320	320×300×12×21
II-2	IPE550	550×210×11×17	126×413×42	HEB360	360×300×13×23

Table 2 Connection characteristics of models employed in the parametric studies

European codes only allow connections which develop extensive yielding at the RBS, through the provision of doubler and continuity plates (e.g. Figure 1b,c), whilst the PZ is expected to refrain from excessive plastic deformations (Castro et al., 2008). In contrast, US design procedures permit some flexibility in the PZ as it may delay strength and stiffness degradation of the plastic hinge formed in the RBS and enhance overall seismic performance of MRFs. It is worth noting that not all connections modelled comply with the Eurocode 8 requirements in terms of the column-to-beam moment ratio, and they are not provided with stiffening elements at the PZ. However, the M-θ in Figures 4a-f allow for qualitative observations regarding the behaviour of main connection components, and recommendations for practical application of non-stiffened panel zones, to be provided. These figures illustrate M-θ curve up to the cycles at which the capacity dropped by more than 15% from the peak (marked with dashed curves). Considering that the yield rotations varied in the range θ_y=6-9 mrad, except for Connection II-2 (Figure 4f) the plastic rotations of all connections were above θ_p=50 mrad indicating reliable levels of ductility, above Eurocode 8 requirements (25 mrad for DCM and 35 mrad for DCH).

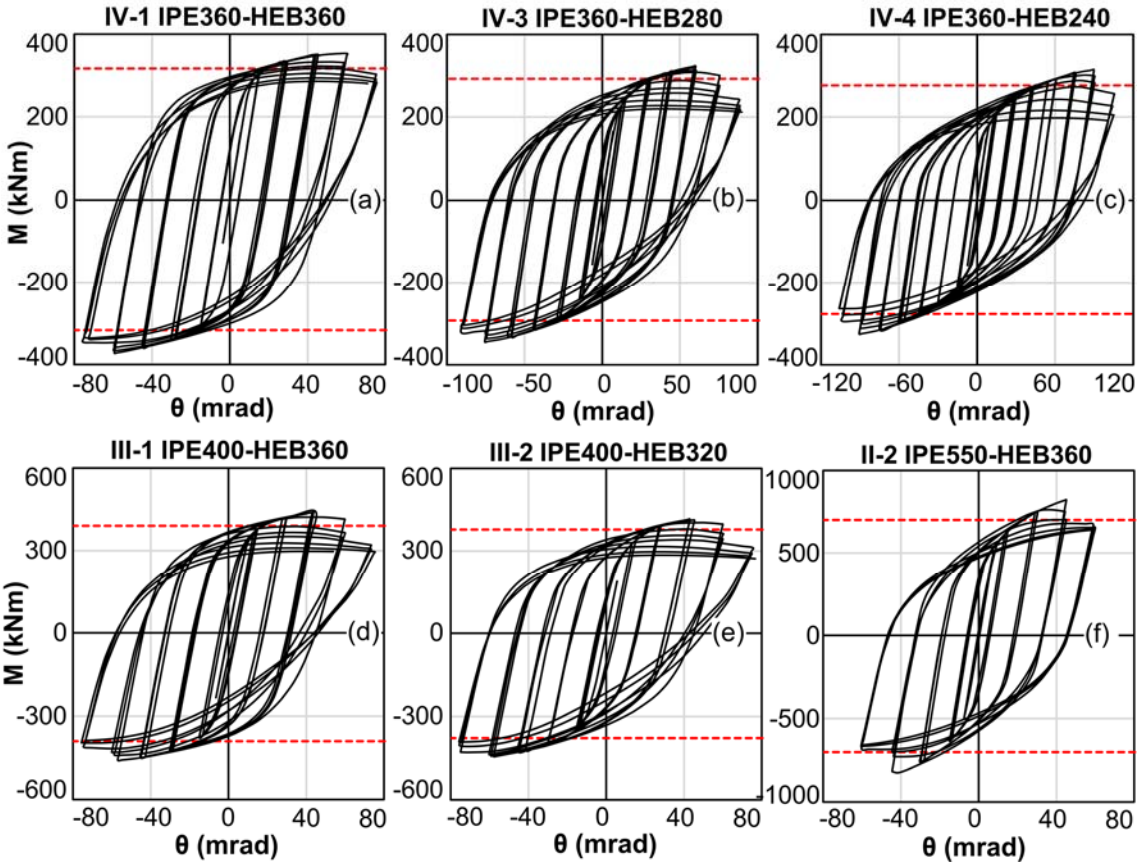

Figure 4 Moment-rotation curves

As observed, all connections developed reliable behaviour with stable inelastic hysteretic response and significant levels of ductility. Generally, the response was characterised by initiation of yielding at the RBS, followed by yielding at the PZ and buckling of the compression flange at the RBS (Figure 4a,b,d,e). A relatively non-symmetric hysteretic response is observed in the unloading positive branch of the M-θ curve after peak, indicating a buckling-triggered strength degradation. Such response is desirable and points out to reliable dissipative behaviour that can be obtained without the provision of continuity or doubler plates at the PZ. As illustrated in Figure 4c,f, the M-θ curves also present a stable hysteretic response. For these connections, the PZ showed excessive distortions with minimal yielding at the RBS. To this end, Figure 5 depicts contributions of the RBS and column web PZ obtained from numerical simulations. The rotation at the RBS was assessed from the relative displacements of the top and bottom RBS cuts, and divided by the beam depths. The column web rotation was determined from the resulting relative web displacements and relative vertical panel displacements (Augusto et al., 2017).

As shown in previous studies, the column provides a minor contribution to the total energy dissipated by the connection under cyclic loading; hence, for the assessments in this paper, its contribution was not considered. For models depicted in Figure 5a-d, most of the rotation was concentrated at the RBS with some contribution from the PZ, whilst the strength degradation primarily occurred due to buckling. As indicated by the panels in the bottom right of each figure, the ratio of the energy dissipated by the RBS/PZ varies between 93/7-62/38 (in %). Although the energy dissipation ratio RBS/PZ = 51/49 for the connection in Figure 5e, this connection had also a reliable cyclic response with rotation θ (at the maximum moment M_u) of 89.6 mrad. This corresponds to a ductility ratio (θ_u/θ_y) of about 10. However, as indicated in the strain map in Figure 5e, some yielding occurred both in the beam and column flanges at the beam-to-column connections suggesting that such RBS/PZ ratios may excessively stress the welds at the column face possibly promoting weld fractures, similar to Specimen C3B described previously.

Model	V_y (kN)	$M_{pl,beam}$ (kNm)	$M_{pl,RBS}$ (kNm)	$V_{max,num}$ (kN)	$M_{max,num}$ (kNm)	F_{max} (kN)	$V_{max,num}$ / V_y (-)	$M_{max,num}$ / $M_{pl,RBS}$ (kNm)	$M_{pl,column}$ / $M_{pl,RBS}$ (-)
IV-1	1242	362	255	827	353	480	0.67	1.38	3.73
IV-3	842	362	255	600	323	338	0.71	1.27	2.13
IV-4	681	362	255	969	314	295	1.42	1.23	1.46
III-1	1242	464	331	869	441	534	0.70	1.34	2.88
III-2	1061	464	331	720	415	465	0.68	1.26	2.31
II-2	1242	989	716	1409	822	1507	1.13	1.15	1.33

Table 3 Comparative results

In contrast to the above, the connection in Figure 5f had an unreliable response in which all 97% of the deformations were concentrated at the PZ. Although its M-θ, depicted in Figure 4f, shows reliable levels of ductility, the strength degradation occurred due to column web buckling as a consequence of the force induced from the beam flanges, resulting in the formation of kinks in the column flanges, hence an undesirable column performance (Castro el al., 2005). This is also indicated by the $V_{max,num}/V_y$ ratios and F_{max} in Table 3, in which $V_{max,num}$ was determined by integrating the shear stresses τ from the centre of the web panel (Figure 6) across its length, as obtained from simulations, whilst V_y was assessed using Eurocode 3 recommendations. The force F_{max} was obtained from the normal stresses σ at the column web resulting from actions induced from the beam flanges. The comparative results in Table 3, also substantiate the qualitative observations regarding Models IV-4 and II-2, as the column-to-RBS plastic moment ratio $M_{pl,column}/M_{pl,RBS}$ has the lowest values from all connections investigated.

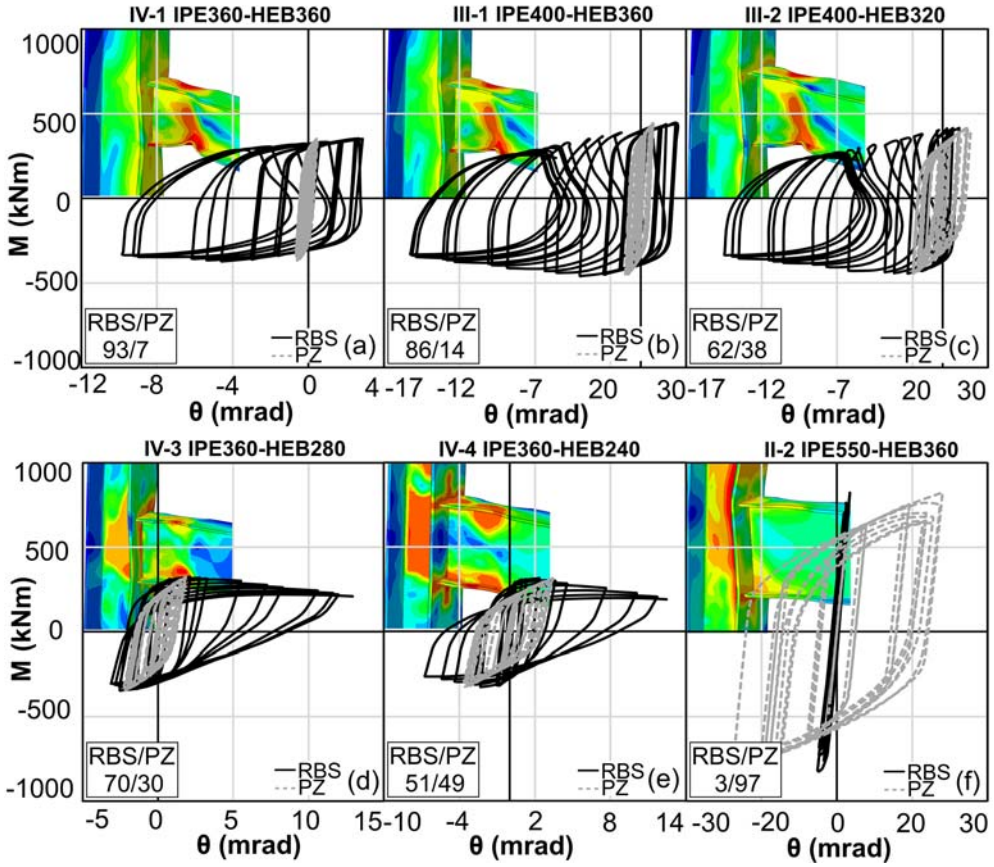

Figure 5 Response of connection components (RBS versus PZ)

Figure 6 illustrates the shear τ and normal σ stresses in the web column panel extracted form simulations along two nodal paths for increments corresponding to peak positive applied displacements. It is observed that the σ values are below yield, whilst τ values are above yield in some cases. Although local shear yielding occurred at the centre of the PZ, the shear plastic capacity of the PZ was not reached (Table 3). As the yielding developed within the RBS, the shear stresses τ decreased in the web column panel to about half of the yield. This is observed in both models from Figure 6, which had a distinct RBS/PZ ratio, indicating that the PZ can be considered as an effective component when energy dissipation is sought. An RBS/PZ ratio up to 65/35 determined by ratios of $V_{max,num} / V_y > 1.0$ and $M_{pl,column} / M_{pl,RBS} > 1.5$ seem to offer a reliable connection behaviour in which the excessive panel zone distortion is limited, and a significant level of energy is dissipated through this component. Such response can generally contribute to relieving the demand on other structural elements, yet it must however be considered with care since large panel deformations may impair the overall structural response as it may be coupled with significant second-order effects (Castro et al., 2005).

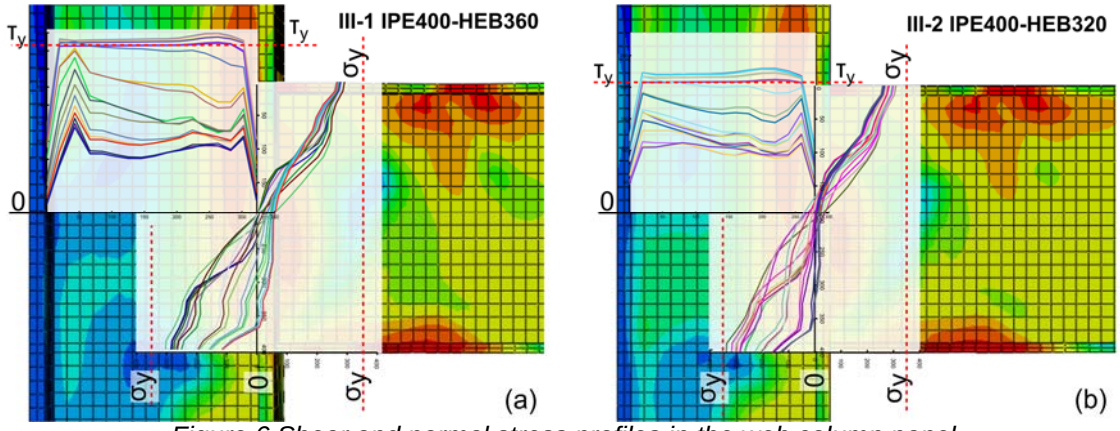

Figure 6 Shear and normal stress profiles in the web column panel

Concluding remarks

This study focused on the non-linear response of RBS beam-to-column connections subjected to cyclic loading. After undertaking numerical validation studies on three specimens from different experimental programmes, parametric investigations were carried out in order to provide detailed insights into the physical behaviour of such connections. Within the parametric investigations, detailed assessments were carried out to examine the contribution of the main connection components to the global response of the connection. Key observations from the numerical simulations have enabled several practical considerations regarding the design of RBS connections to be highlighted.

Detailed non-linear models can estimate reliably the characteristic response of beam-to-column connections incorporating reduced beam sections, including the stiffness, strength, post-yield stress distribution between connection components as well as the post-peak strength degradation. Strain maps from numerical validations indicate that local effects such as flange and web buckling at the reduced beam section as well as column web panel distortion are well predicted when precise material characteristics combined with a relatively refined mesh are considered in modelling. Qualitative observations from the validations indicate that straight-cut reduced beam sections may not ensure a ductile connection response, primarily due to extreme strain localisations at the column face, whilst reduced sections with radius-cut forms may act as reliable limiting mechanisms for excessive deformations in the column and non-stiffened panel zones. As expected, the presence of doubler and continuity plates at the column panel zone, as recommended by current European seismic provisions, increase the rigidity of the connection and facilitate stress concentrations at the reduced beam section, restraining the panel zone from excessive plastic deformations.

As some flexibility within the panel zone can contribute to reducing the demand on other structural elements, some energy dissipation through this component can enhance the performance of moment resisting frames. The results of the parametric studies showed that the response of connections incorporating non-stiffened panel zones depends on the section sizes of the connection components, whilst the inelastic behaviour is determined by the energy dissipated

through these components. Although some connections exhibited stable hysteretic response with ductility ratios around ten, extensive yielding occurred at both key components and was combined with strain localisation at the column face, which could promote weld fractures. These connections had a reduced beam section-to-panel zone energy dissipation ratio of about 50/50 and may be rendered as unreliable as they may impair the overall structural response of moment resisting frames. Connections with reduced beam section-to-panel zone energy dissipation ratios in the range of 65/35-100/0, which can be obtained by ensuring a panel zone with a shear plastic capacity higher than the shear demand, and with a plastic moment column capacity of at least 50% greater than that at the reduced beam section, seem to offer effective configurations as they develop a stable hysteretic response with a significant level of ductility. In such cases, the local flange buckling occurring at the reduced beam section acts as a limiting mechanism for the extensive hardening that would occur for connections with energy dissipation ratio of about 50/50.

Acknowledgements

The financial support of the Research Fund for Coal and Steel of the European Community within the project EQUALJOINTS-PLUS, Grant agreement no 754048 (2017), for the investigations described in this paper is gratefully acknowledged.

References

Augusto H, Simões da Silva L, Rebelo C, Castro JM (2017), Cyclic behaviour characterization of web panel components in bolted end-plate steel joints, *Journal of Constructional Steel Research*, 133: 310-333.

ANSI/AISC 358-05 *Prequalified Connections for Special and Intermediate Steel Moment Frames for Seismic Applications.*

EN 1993-1-1:2005, *Eurocode 3: Design of steel structures - Part 1-1: General rules and rules for buildings.*

EN 1993-1-8:2005, *Eurocode 3: Design of steel structures - Part 1-8: Design of joints*

EN 1998-1:2004, *Eurocode 8: Design of structures for earthquake resistance – Part 1: General rules, seismic actions and rules for buildings.*

EN 1998-3:2005*, Eurocode 8: Design of structures for earthquake resistance – Part 3: Assessment and retrofitting of buildings.*

Bogdan T, Bompa DV, Elghazouli AY, Nunez E, Leon R (2019), Experimental and numerical simulations on RBS connections incorporating large sections. To be presented *in Papadrakakis and Fragiadakis (eds.), COMPDYN 2019 7th ECCOMAS Thematic Conference on Computational Methods in Structural Dynamics and Earthquake Engineering,* Crete, Greece, 24–26 June 2019.

Bompa DV and Elghazouli AY (2017), Numerical modelling and parametric assessment of hybrid flat slabs with steel shear heads, *Engineering Structures*, 142: 67-83.

Castro JM, Dávila-Arbona FJ, Elghazouli AY (2008), Seismic design approaches for panel zones in steel moment frames, *Journal of Earthquake Engineering*, 12: 34-51.

Castro JM, Elghazouli AY, Izzuddin BA (2005), Modelling of the panel zone in steel and composite moment frames, *Engineering Structures*, 27(1): 129-144.

Chen S, Yeh C, Chu J (1996), Ductile steel beam-to-column connections for seismic resistance, *Journal of Structural Engineering,* 121(11): 1292-1299.

Chen S and Tu C (2004), Experimental study of jumbo size reduced beam section connections using high-strength steel, *Journal of Structural Engineering,* 130(4): 582-587.

Chi B and Uang C (2002), Cyclic response and design recommendations of reduced beam section moment connections with deep columns, *Journal of Structural Engineering,* 128(4): 464-473.

Dassault Systèmes Simulia Corp (2014), *ABAQUS Analysis user's manual* 6.14, DSS.

Elghazouli AY (2015), Seismic Code Developments for Steel and Composite Structures. *In: Ansal A. (eds) Perspectives on European Earthquake Engineering and Seismology. Geotechnical, Geological and Earthquake Engineering,* vol 39. Springer, Cham.

Engelhardt MD, Winneberger T, Zekany AJ, Potyraj TJ (1996), The dogbone connection: Part II. *Modern Steel Construction,* 36 (8): 46-55.

Jones SL, Fry GT, Engelhardt MD (2002), Experimental Evaluation of Cyclically Loaded Reduced Beam Section Moment Connections, *Journal of Structural Engineering*, 128(4): 441-451.

Landolfo R, D'Aniello M, Costanzo S, Tartaglia R, Stratan R, Dubina D, Vulcu C, Maris C, Zub C, Simões da Silva L, Rebelo C, Augusto H, Shahbazian A, Gentili F, Jaspart JP, Demonceau JF, Hoang LV, Elghazouli AY, Tsitos A, Vassart O, Moreno Nunez E, Dehan V, Hamreza C (2018) *European pre-QUALified steel JOINTS (EQUALJOINTS), Final Report*, 2018-05-04, Directorate-General for Research and In-novation (European Commission). Available at: https://publications.europa.eu/s/j7q0 (Accessed 7/01/2019).

Lee CH, Jeon SW, Kim JH, Uang CM (2005), *Effects of panel zone strength on seismic performance of reduced beam section steel moment connections.* Asian-Pacific Network of Centers for Earthquake Engineering Research (ANCER).

Qi L, Paquette J, Eatherthon M, Leon R, Bogdan T, Popa N, Nunez Moreno E (2018), Analysis of Fracture Behaviour of Large Steel Beam Column Connections, *In 12th Inter-national Conference on Advances in Steel-Concrete Composite Structures (ASCCS).*

Pachoumis DT, Galoussis EG, Kalfas CN, Christitsas AD (2009), Reduced beam section moment connections subjected to cyclic loading: Experimental analysis and FEM simulation, *Engineering Structures,* 31: 216-223.

Pachoumis D, Galoussis, EG, Kalfas CN, Efthimiou IZ (2010), Cyclic performance of steel moment-resisting connections with reduced beam sections—experimental analysis and finite element model simulation, *Engineering Structures,* 32(9): 2683-2692.

Plumier A (1990), New idea for safe structures in seismic zones. In *IABSE Symposium-Mixed Structures Including New Materials*.

Plumier A, Beg D, Sanchez L (2000) *Influence of strain rate*, Test report, Université de Liège

Popov E, Blondet M, Stepanov L, Stojadinovic B (1996), *Full-Scale Beam-to column connection tests,* University of California Department of Civil Engineering, Berkeley, CA.

SAC (1995) *Survey and assessment of damage to buildings affected by the Northridge Earthquake of January 17, 1994,* SAC95-06, SAC Joint Venture, Sacramento.

Sofias CE, Kalfas CN, Pachoumis DT (2013) Experimental and FEM analysis of reduced beam section moment endplate connections under cyclic loading, *Engineering Structures*, 59(2014): 320-329.

Vulcu C, Stratan A, Ciutina A, Dubina D (2017), Beam-to-CFT high-strength joints with external diaphragm. II: Numerical simulation of joint behavior. *Journal of Structural Engineering*, 143(5): 04017002.

Zhang X and Ricles JM (2006) Seismic behavior of reduced beam section moment connections to deep columns, *Journal of Structural Engineering,* 132(3): 358-367.